HAL
open science

Mesenchymal Stem Cell Features of Ewing Tumors

Franck Tirode, Karine Laud-Duval, Alexandre Prieur, Bruno Delorme, Pierre Charbord, Olivier Delattre

To cite this version:

Franck Tirode, Karine Laud-Duval, Alexandre Prieur, Bruno Delorme, Pierre Charbord, et al.. Mesenchymal Stem Cell Features of Ewing Tumors. Cancer Cell, 2007, 11 (5), pp.421-429. 10.1016/j.ccr.2007.02.027 . inserm-02438637

HAL Id: inserm-02438637

https://inserm.hal.science/inserm-02438637v1

Submitted on 14 Jan 2020

HAL is a multi-disciplinary open access archive for the deposit and dissemination of scientific research documents, whether they are published or not. The documents may come from teaching and research institutions in France or abroad, or from public or private research centers.

L'archive ouverte pluridisciplinaire **HAL**, est destinée au dépôt et à la diffusion de documents scientifiques de niveau recherche, publiés ou non, émanant des établissements d'enseignement et de recherche français ou étrangers, des laboratoires publics ou privés.

A-PDF MERGER DEMO

Mesenchymal stem cell features of Ewing tumors

Franck Tirode [1,2], Karine Laud-Duval [1,2], Alexandre Prieur [1,2], Bruno Delorme [3], Pierre Charbord [3] and Olivier Delattre [1,2,*]

[1] Institut Curie, 26 rue d'Ulm, 75248 Paris cedex 05, France

[2] INSERM, U830, Unité de Génétique et Biologie des Cancers, Paris, France

[3] INSERM, ESPRI/EA3855, Microenvironnement de l'Hématopoièse et Cellules Souches, Faculté de Médecine de Tours, 10 Bd Tonnellé, 37032 Tours cedex 1, France

[*] Corresponding author

Olivier Delattre, INSERMU830, Section de Recherche, Institut Curie, 26 rue d'Ulm, 75248 Paris Cedex 05
Tel: 33 1 42 34 66 81
Fax: 33 1 42 34 66 30
Email: olivier.delattre@curie.fr

Summary

The cellular origin of Ewing tumor (ET), a tumor of bone or soft tissues characterized by specific fusions between *EWS* and *ETS* genes, is highly debated. Through gene expression analysis comparing ETs with a variety of normal tissues, we show that the profiles of different *EWS-FLI1*-silenced Ewing cell lines converge toward that of mesenchymal stem cells (MSC). Moreover, upon *EWS-FLI1* silencing, two different Ewing cell lines can differentiate along the adipogenic lineage when incubated in appropriate differentiation cocktails. In addition, Ewing cells can also differentiate along the osteogenic lineage upon long-term inhibition of *EWS-FLI1*. These *in silico* and experimental data strongly suggest that the inhibition of *EWS-FLI1* may allow Ewing cells to recover the phenotype of their MSC progenitor.

Significance

The precise knowledge of the normal counterpart of cancer cells is dramatically lacking for Ewing sarcoma, one of the most frequent primary bone tumors. Since its initial description more than 80 years ago, endothelial, epithelial, neural and mesenchymal origins have been hypothesized. We have developed original cell models to regulate *EWS-FLI1* expression. *In silico* analyses and *in vitro* differentiation experiments provide strong evidences that Ewing tumors originate from a mesenchymal precursor that may have both connective and vascular differentiation potentials. This origin helps to clarify the issue of the predominant localization of ET in bone or soft tissue, two tissues that constitute major sources of MSC.

Introduction

Ewing tumor (ET), the second most frequent bone tumor in adolescent and young adult, harbors characteristic translocations which fuse the 5' portion of the *EWS* gene with the 3' region, encoding DNA binding domain, of one of five *ETS* family genes (Arvand and Denny, 2001; Janknecht, 2005). The specificity of these translocations for ET has now been extensively documented. The most frequent fusion occurs with the *FLI1* gene as a consequence of the t(11;22)(q24;q12) translocation (Delattre et al., 1992). The resulting *EWS-FLI1* chimeric protein behaves as an aberrant transcription regulator that is thought to induce transformation through induction or repression of specific target genes. Accordingly, a number of genes controlling cell growth, signal transduction or differentiation have been shown to be regulated by *EWS-FLI1* (reviewed in Janknecht, 2005).

Histologically, ET appears as uniformly undifferentiated small round cells containing a vesicular nuclei and a small cytoplasm within a sparse intercellular stroma. These characteristics are poorly indicative of the cell lineage that gives rise to ET. Since the initial proposal of an endothelial origin by James Ewing in 1921 (Ewing, 1921), the issue of the ET progenitor is highly debated. A neural crest origin is hypothesized by the observation that *EWS-ETS* fusions characterize a spectrum of tumors with undifferentiated ETs at one end and differentiated peripheral primitive neuroectodermal tumors, expressing various neural markers, at the other end. This hypothesis is further strengthened by the observation that ET derived cell lines grown *in vitro* can undergo neural differentiation upon treatment with various differentiation-inducing agents (Cavazzana et al., 1987; Noguera et al., 1994). A recent study suggests that *EWS-FLI1* expression itself may be responsible, at least in part, for the observed primitive neuroectodermal phenotype of ET through the regulation of neural

specific genes (Hu-Lieskovan et al., 2005). This study indicates that the ultimate phenotype of ET might be determined not only by the cell lineage from which it derives but also by intrinsic effects of *EWS-FLI1*. *EWS-FLI1* has also been shown to inhibit neural differentiation of neuroblastoma cells therefore leading to the proposal that *EWS-FLI1* may shift the sympathetic differentiation program of neuroblastoma to the parasympathetic one of ET (Rorie et al., 2004).

Other experiments indicate that *EWS-FLI1* inhibits mesenchymal differentiation. In particular, enforced expression of *EWS-FLI1* inhibits adipogenic and osteogenic differentiation in murine marrow stromal cells (Torchia et al., 2003). It also impairs myogenic differentiation in C2C12 myoblasts (Eliazer et al., 2003). The hypothesis of a mesenchymal origin of ET is further supported by two recent reports indicating that *EWS-FLI1* can transform primary bone marrow stromal cells and induce the formation of tumors resembling Ewing sarcomas in SCID mice (Castillero-Trejo et al., 2005; Riggi et al., 2005). This indicates that, unlike other cell types which cannot be transformed by *EWS-FLI1* alone and necessitate additional events, mesenchymal stem cells display permissiveness for *EWS-FLI1*-mediated cell transformation and may therefore constitute an appropriate background for ET development.

Finally, together with the observation of occasional cytokeratin staining, the study of tight junction structural proteins has suggested that ETs exhibit partial epithelial differentiation (Schuetz et al., 2005).

Presently, all attempts to identify the ET cell of origin have relied on the overexpression of *EWS-FLI1* in various heterologous backgrounds. In this study, we have tested the hypothesis that Ewing cells, inhibited for *EWS-FLI1* by a specific

small hairpin RNA (shRNA), may recover characteristics of their primary origin and responsiveness to differentiation programs.

Experimental Procedures

Inhibition of *EWS-FLI1*

A673 and SK-N-MC were obtained from ATCC. EW24 derived from a bone tumour was kindly provided by Pr Gilbert Lenoir (Zucman et al., 1993). All three cell lines exhibit a type 1 fusion transcript. For siRNA mediated silencing, A673 Ewing cells expressing a type 1 fusion transcript were transfected mainly as previously described (Prieur et al., 2004), except that transfection medium was removed 6 hours after transfection instead of 24 hours and replaced by fresh medium changed every two days. For doxycycline inducible silencing, the oligonucleotides of the *EWS-FLI1* short hairpin RNAs (shEF-1) 5'GATCCCGGCAGCAGAACCCTTCTTAttcaagagaTAAGAAGGGTTCTGCTGCCTTTTTGGAAA3' (sense) and 5'GGCCGTCGTCGTCTTGGGAAGAATaagttctctATTCTTCCCAAGACGACGGAAAAACCTTTTCGA3' (antisense) were annealed and then cloned between the *Bgl*II and *Hind*III restriction sites of the pTER vector (van de Wetering et al., 2003). Expression plasmids were transfected in A673 Ewing cell line with the effectene transfection reagent (Qiagen, Paris, France) according to the manufacturer's instructions. A Tet repressor expressing clone (A673tetR5BIII) was selected on Blasticidine (20µg/mL) then transfected with the pTER/shEF-1 construct encoding Zeocin resistance (200µg/mL). Two clones (shA673-1C and -2C), exhibiting strong inhibition of *EWS-FLI1* upon treatment with 1µg/mL Doxycycline (DOX), were selected. For lentivirus-mediated silencing of EW24 and SK-N-MC cell lines, the H1 promoter-tetO-shEF-1 cassette from pTER/shEF-1 vector was inserted in the pTRIP lentiviral expression vector. Packaging and titration using GFP as a reporter were performed according to the tronolab website (http://tronolab.epfl.ch/).

Isolation of human bone marrow stromal cells (BMSC).

Human primary BMSCs were obtained after informed consent from bone marrow aspirates (iliac crest) of patients undergoing hip replacement surgery. Mononuclear cells were plated at the density of 50 000 cells/cm^2 and cultured in α-MEM without nucleotides (Gibco BRL, Invitrogen, Cergy-Pontoise, France), supplemented with 10% FCS (Hyclone), L-glutamine 2 mM (Gibco BRL) and 1ng/mL bFGF (AbCys). After two weeks, confluent cells were detached with trypsin/EDTA and replated at 1000 cells/cm^2 (passage 1, P1). Cells were phenotyped as BMSC by flow cytometry (negative for CD34, CD31 and CD45 and positive for CD73, CD90, CD105 and CD44). The three-lineages (adipocyte, osteocyte, and chondrocyte) differentiation potential of these cells was controlled.

Isolation of RNAs and microarray analyses.

Total RNAs were isolated using the Trizol Reagent (Invitrogen). RNAs were isolated 9 days following transfection of A673 Ewing cells with the specific *EWS-FLI1* siRNA (siEF1) or with the control siRNA (siCT) and 3 days after infection of EW24 and SK-N-MC with lentiviruses encoding *EWS-FLI1*-specific or control shRNA. RNAs from 27 ET samples and from freshly isolated (P1) BMSCs were also used for microarray analyses. Experimental procedures for GeneChip microarray were performed according to the Affymetrix GeneChip Expression Analysis Technical Manual (Affymetrix, Santa Clara, CA) using HG-U133A arrays. CEL files from E-AFMX-5 (Su et al., 2004) and from E-MEXP-167 and E-MEXP-168 (Boquest et al., 2005) datasets were downloaded from the EBI's ArrayExpress repository (Parkinson et al., 2005). Additional CEL files for *EWS-FLI1*-silenced A673 cells were kindly provided by Steve Lessnick (Smith et al., 2006). All microarray data were simultaneously normalized using the gcrma package version 1.1.4 in the R environment (R Development Core

Team, 2005). Principal component analyses were performed using the PCA tool of MeV TM4 software (Saeed et al., 2003). SAM analyses were performed with the samr package version 1.22 (Tusher et al., 2001). Microarray data are available at Gene Expression Omnibus (GEO; http://www.ncbi.nlm.nih.gov/geo/) public database with the accession number GSE7007.

Real-time quantitative reverse transcription-PCR.

cDNAs were synthesized from 1µg of RNA using the GeneAmp RNA PCR core Kit (Applied Biosystem, Courtaboeuf, France). Quantitative PCR analyses were performed using TaqMan Assays-on-demand Gene expression reagents (Applied Biosystem) with qPCR Mastermix Plus without UNG (Eurogentec, Belgium). Reactions were run on an ABI/PRISM 7500 (Applied Biosystem) and analyzed using the 7500 system SDS software. The following Assays-on-demand were used: *FABP4* (Hs00609791_m1); *LPL* (Hs00173425_m1); *PPARG* (Hs00234592_m1); *ALPL* (Hs00758162_m1); *RUNX2* (Hs00231692_m1); *SPP1* (Hs00167093_m1); *SOX9* (Hs00165814_m1); *COL10A1* (Hs00166657_m1), *PAX7* (Hs00242962_m1), *FOXD3* (Hs00255287_m1), *SNAI2* (Hs00161904_m1) and *RPLP0* (Hs99999902_m1). *RPLP0* expression, which does not vary upon shRNA induction or differentiation conditions, was used for normalization. *EWS-FLI1* expression was quantified by SYBR green (Applied Biosystem) using the following primers: forward 5'GAGGCCAGAATTCATGTTATTGC3'; reverse 5'GCCAAGCTCCAAGTCAATATAGC3'.

Cell cycle analyses by flow cytometry

Cell cycle analyses were performed by BrdU incorporation as previously described (Dauphinot et al., 2001). Samples were subjected to FACS analysis (FACScalibur, BD Biosciences, San Diego, USA) and the data were processed using CELL Quest

software (BD Biosciences). For cell surface markers detection, 10^5 cells were incubated 30 min at 4°C in 100 µL of PBS with phycoerythrin (PE)-conjugated mAb. Cells were then washed twice and then proceeded immediately for FACS analysis. The PE-conjugated antibodies from BD Biosciences used were: IgG1-PE (MOPC-2), CD29-PE (MAR4), CD31-PE (WM59), CD44-PE (G44-26), CD45-PE (HI30), CD54-PE (HA58), CD59-PE (H19), CD90-PE (5E10) and CD166-PE (3A6). CD105-PE (SN6) was from Invitrogen.

Differentiation assays.

For adipogenic differentiation, cells were plated and grown for 2 days at 37°C, 5% CO_2 in DMEM or RPMI containing 10% FCS, 0.5mM IsoButylMethylXanthine (Sigma), 1µM dexamethasone (Sigma) and 10µg/mL Insulin (Sigma). Medium was then replaced by DMEM or RPMI, 10% FCS, with 10µg/mL Insulin and cells were grown for six additional days with medium changes every two days, then collected for quantitative-RT-PCR or fixed in 4% paraformaldehyde (Sigma) prior to staining with 0.3% w/v Oil-Red-O (Sigma) in 60% isopropanol. For osteogenic differentiation, cells were grown in DMEM, 10% serum, 0.1µM dexamethasone, 0.15mM L-ascorbic acid (Sigma), 2mM β-glycerophosphate (Sigma) and 1mM NaH_2PO_4 for 21 days. Paraformaldehyde fixed calcium depositions were stained by the Von-Kossa protocol including incubation with 5% silver nitrate (Sigma) for 30 min, extensive washing with PBS, exposition for 20 min to UV and incubation in 5% sodium thiosulfate for 5 min. For chondrogenic differentiation, cells were grown in pellet as previously described (Johnstone et al., 1998). Briefly, $4x10^5$ cells centrifuged 5 min at 1200 rpm in a 15-ml polypropylene tube were grown in pellet in 500µl of DMEM without serum but containing 0.1µM dexamethasone, 0.15mM L-ascorbic acid, 0.35 mM proline, 1mM

sodium pyruvate, 1x ITS (Roche, Meylan, France), 10ng/mL TGFβ3 (R&D system, Lille, France), and 10ng/mL IGF1 (Abcys) for 21 days.

Results

Convergence of *EWS-FLI1*-silenced Ewing cells toward mesenchymal stem cells *in silico*

To gain insight into the origin of Ewing tumors (ET), we compared the expression profile of 27 ETs with that of various normal human tissues (Su et al., 2004), human Mesenchymal Stem Cells (MSCs) (Boquest et al., 2005) and freshly prepared Bone Marrow Stromal Cells (BMSC). This dataset hence contained different tissues from neural (central or peripheral), epithelial, hematopoietic or mesenchymal origins. Duplicate data, obtained with three Ewing cell lines silenced for *EWS-FLI1* expression by RNA interference, were also included in this *in-silico* analysis. These silencing experiments were initially performed with an *EWS-FLI1*-specific siRNA for the A673 cell line which can be efficiently transfected (Prieur et al.2004). Given the low efficiency of such transfection in other cell lines, we developed lentiviral vectors to express a shRNA corresponding to the junction between *EWS* and *FLI1* genes. This lentivirus was used to infect EW24 and SK-N-MC cells. In addition, data recently published for *EWS-FLI1*-silenced A673 cells (Smith et al., 2006) were also included in this analysis (a complete description of the whole dataset is provided in Table S1). All experiments, performed on Affymetrix HG-U133A chips, were simultaneously normalized using gcrma. Hierarchical clustering and principal component analyses (PCA) using all probe sets showed that ETs clustered, together *EWS-FLI1*-silenced (efRNAi) and control (ctrlRNAi) samples, apart from all other tissues. This indicated that ET form a homogeneous group not evidently related to any normal tissue (Figure 1A). Based on the hypothesis that *EWS-FLI1* may modulate differentiation genes, we performed a new PCA analysis with genes strongly and significantly modulated by *EWS-FLI1* as identified by SAM analysis comparing efRNAi and ctrlRNAi samples.

As shown in figure 1B, ETs were still clustered with ctrlRNAi apart from other tissues. In contrast, efRNAi samples shifted away from the ET cluster to join the mesenchymal group containing undifferentiated BMSCs or MSCs but also the more differentiated adipocytes and myocytes. Hierarchical clustering analysis using the same probesets also enabled to visualize the vicinity of efRNAi with tissues derived from the mesenchymal lineage (Figure 1C and Figure S1). These *in silico* analyses provided a first clue that *EWS-FLI1* may regulate a subset of genes involved in mesenchymal commitment or differentiation.

We more precisely investigated similarities between genes modulated by *EWS-FLI1* in Ewing cell lines and genes differentially expressed between MSCs and Ewing tumors. SAM analyses enabled the identification of 3238 probe sets (2430 genes) differently expressed between MSCs and ETs (absolute fold change>2; q-values < 10^{-2})(Table S2). Comparisons of MSCs/ETs genesets with the 289 genes identified between efRNAi and ctrlRNAi using the same criteria demonstrated a very significant overlap of 110 genes ($p< 10^{-16}$, exact binomial test) (Table S2). Most of these genes behaved in a consistent manner between both comparisons, genes downregulated by *EWS-FLI1* being overexpressed in MSCs as compared to ETs and genes upregulated by *EWS-FLI1* being underexpressed in MSCs (Figure 1D). We next investigated gene sets specifically modulated by *EWS-FLI1* in each individual cell lines. As expected, for each cell line, the overlap between MSCs/ETs-differential genes and *EWS-FLI1*-regulated genes was highly significant although it was larger for A673. In addition to a common core set of genes regulated by *EWS-FLI1* in all three cell lines, this analysis pointed out cell line-specific genesets (Figure 1E and Table S2). Among genes common to the MSC/ET comparison and regulated by *EWS-FLI1* in at least 2 of the Ewing cell lines (grey area in Figure 1E), various

signaling molecules (DKK1, IGFBPs, CYR61) are key regulators of pathways controlling the commitment of MSCs to different lineages (Kiepe et al., 2006; Schutze et al., 2005; van der Horst et al., 2005). The overlap also contains numerous genes whose products are involved in the cytoskeleton and matrix remodeling associated with mesenchymal cell biology (Table 1). In agreement with the proposed endothelial potential of MSCs, some genes modulated by *EWS-FLI1* and expressed by MSCs have critical role in angiogenesis (Table 1). Finally, the inhibition of *EWS-FLI1* also induced the expression of some master genes of the mesenchymal differentiation (including *SOX9* and *BMP1*) that are not expressed in undifferentiated MSCs. Together, these results strongly suggested that the *EWS-FLI1*-silenced Ewing cells recover an expression pattern related to that of MSCs. They also showed that a number of neural genes expressed in ETs, but not in MSCs, are regulated by *EWS-FLI1* (Table 1).

***EWS-FLI1*-silenced Ewing cells harbor mesenchymal features.**

From these *in silico* analyses, we postulated that terminal differentiation in the mesenchymal lineages might be achieved upon combined effects of *EWS-FLI1* silencing and treatment of cells with appropriate differentiation cocktails. To test this hypothesis, *EWS-FLI1* silenced EW24, SK-N-MC and A673 cells were used to conduct *in vitro* adipogenic differentiation experiments (Figure 2). Upon differentiation conditions, EW24 infected with the control lentivirus and hence harboring a normal *EWS-FLI1* expression exhibited a mild induction of *PPARγ2* and *FABP4* and a strong induction of *LPL*, three specific markers of the adipocyte lineage (Figure 2A). The silencing of *EWS-FLI1* in EW24 cells grown in standard or differentiation media led to a much stronger induction of *FABP4* and to a lesser extent of *PPARγ2*. Oil-Red-O

staining, which labels lipidic vesicles, was not significant for EW24 infected with the control virus either in basal or differentiation conditions. The inhibition of *EWS-FLI1* by itself induced a light Oil-Red-O staining of a few cells (Figure 3B). However, this staining was much more obvious when *EWS-FLI1*-silenced cells were incubated in the presence of differentiation medium (Figure 2B). These results indicated that EW24 cells exhibit some degree of adipogenic conversion upon incubation with specific cocktail or upon *EWS-FLI1* silencing but that this commitment is much more pronounced when both conditions are combined. A similar observation was made with A673 (data not shown and see below). In contrast, neither induction of markers, nor Oil-Red-O staining was observed in the SK-N-MC cell line.

In addition to adipogenic differentiation, MSC can also commit to the osteogenic or chondrogenic lineages. However, these differentiations necessitate up to several weeks of incubation with specific media, which is hardly compatible with the si or shRNA approaches used in the previous experiments. Indeed, due to a progressive overgrowth of poorly inhibited cells, a long term and stable *EWS-FLI1* silencing could not be achieved with these systems. To circumvent this technical constrain we constructed Ewing cell lines expressing a doxycycline (DOX) inducible shRNA targeting *EWS-FLI1*. Two independent clones (shA673-1C and -2C) were isolated**.** As shown in figure 3A, the induction of the shRNA led to a dramatic reduction of *EWS-FLI1* transcript and protein levels observed by 24h after addition of DOX in the culture medium and remaining stable over time. In agreement with previous observations based on siRNAs (Chansky et al., 2004; Prieur et al., 2004), inducible *EWS-FLI1* silencing resulted in a considerable decrease of cell proliferation associated with a reduced number of cells in the S-phase of the cell cycle and a simultaneous increase of the amount of G1-phase cells (Figure S2). We first

confirmed that adipogenic differentiation conducted with both inducible clones led to results similar to those described above. In the presence of *EWS-FLI1* (-DOX), differentiation medium led to a significant induction of the three adipogenic markers (Figure 3B). The knock-down of *EWS-FLI1* in standard medium also led to an induction of these transcripts. Nevertheless, the increased expression of these three genes was higher when differentiation was conducted in the presence of DOX, suggesting that inhibition of *EWS-FLI1* and differentiation cocktail may provide additive or even synergistic effects (see *PPARγ2* and *LPL*). Finally, Oil-Red-O staining was positive only for cells treated by both DOX and the differentiation cocktail (Figure 3C). Altogether these data show that *EWS-FLI1*-inhibited Ewing cells can accumulate lipid vesicles and express adipogenic markers, two features highly suggestive of a differentiation along the adipocyte lineage.

Similar experiments were conducted for osteogenic differentiation using quantitative RT-PCR analyses of three markers specific for this lineage (*SPP1*, *ALPL* and *RUNX2*) and Von-Kossa staining. The *EWS-FLI1* silencing and subsequent growth arrest observed with DOX treatment of shA673 cells were stable over time and long-term differentiation experiments could thus be conducted. The three afore-mentioned osteogenic markers were induced by DOX and/or differentiation mix with different patterns. The induction of *ALPL* was clearly dependent upon the medium but not influenced by *EWS-FLI1* (Figure 3D). Contrarily, differentiation medium and DOX exhibited additive or even synergistic effects for *RUNX2* and *SPP1* inductions. Even more strikingly, the Von-Kossa staining of shA673 grown for three weeks in differentiation medium and DOX demonstrated the presence of a calcified matrix whereas this was observed neither in cells grown in differentiation medium without DOX nor in standard medium with or without DOX (Figure 3E). Together these

results show that *EWS-FLI1*-silenced Ewing cells can exhibit characteristic features of osteocytes.

As MSCs are also precursors of chondrocytes, we tested whether shA673 cells could differentiate along this lineage. Pellet cultures of shA673 cells were performed either in presence or absence of DOX and chondrogenic differentiation medium. Whereas *EWS-FLI1*-expressing shA673 cells remained flat and rapidly died, *EWS-FLI1*-silenced shA673 formed a round pellet, but ultimately died prior to the delay necessary to evaluate terminal chondrocyte differentiation. However, quantitative RT-PCR experiments showed that, in addition to the afore-mentioned *RUNX2* induction, *COL10A1* and *SOX9*, two markers of the chondrocyte lineage, were upregulated upon *EWS-FLI1* silencing (Figure 3D). These results suggested that Ewing cells can engage the initial steps of chondrocyte differentiation but cannot fully complete this process.

Finally, since MSCs can be characterized by the expression of several surface antigens (Covas et al., 2005; Izadpanah et al., 2005; Oswald et al., 2004; Pittenger et al., 1999), we investigated the expression of 10 surface markers using FACS analyses in the presence or absence of *EWS-FLI1* (Figure 3F). Five of these (CD44, CD59, CD73, CD29 and CD54) were expressed on shA673 cells and induced by *EWS-FLI1* inhibition. Three (CD90, CD105 and CD166) were expressed but not modified by *EWS-FLI1* modulation. Finally, CD45 and CD31, two markers expressed in hematopoeitic stem cells or endothelial cells, but not in mesenchymal stem cells, were not detected at the surface of Ewing cells whatever the *EWS-FLI1* status. Altogether these results strengthen the hypothesis of *EWS-FLI1*-silenced Ewing cells sharing phenotypic characteristics with MSCs.

Discussion

The fusion between *EWS* and members of the ETS family, usually *FLI1*, is a critical event of Ewing sarcoma development. *EWS-ETS* fusions are only observed in tumors of the Ewing family, suggesting that transformation is dependent upon the specific action of this oncogene within a precise cell background. Consequently, a thorough phenotypic analysis of *EWS-FLI1*-silenced Ewing cells should give insights into this cellular context. We have addressed this issue investigating the transcription profile of *EWS-FLI1*-silenced Ewing cells. Numerous genes involved in neural development and differentiation are expressed in ET and repressed upon inhibition of *EWS-FLI1*. This observation is in complete agreement with the occasional presence of neural markers in ETs and with the recently reported shift from myogenic to neural phenotype induced by *EWS-FLI1* expression in rhabdomyosarcoma cells (Hu-Lieskovan et al., 2005). It confirms that *EWS-FLI1* by itself can promote the induction of some neural crest genes. However, our data show that the neural profile of Ewing cells is not sufficient for ETs to cluster among neural tissues (Figure 1A).

The more striking *in silico* observation is that three different *EWS-FLI1*-inhibited Ewing cell lines cluster with MSCs when the analysis is performed with *EWS-FLI1*-modulated genes. MSCs were initially described by Friedenstein (Friedenstein et al., 1976) who isolated plastic adherent cells from bone marrow capable of differentiating into adipocytes, chondrocytes and osteocytes. More recently, a number of investigators have shown that multi-potent MSCs can be isolated from a variety of sources including bone marrow, adipose tissue, connective tissues, placenta and umbilical cord blood (for review see Dennis and Charbord, 2002; Gregory et al., 2005). In addition to the afore-mentioned lineages, MSCs can also give rise to stromal cells supporting hematopoiesis and also probably to

endothelial and vascular smooth muscle cells. Our study show that markers currently used for the isolation of MSCs may be induced upon *EWS-FLI1* inhibition (CD44, CD54, CD59 and CD73). The *in silico* analysis described above is strongly supported by experiments showing that *EWS-FLI1*-inhibited Ewing cells, but not parental Ewing cells, exhibit differentiation characteristics of mesenchymal lineages. Indeed, two out of three Ewing cell lines can be clearly differentiated along the adipogenic lineage. This indicates that at least in these two cell lines, the apparatus responsible for the adipogenic differentiation is present but impaired by *EWS-FLI1*. Long term inhibition of *EWS-FLI1* also shows that terminal osteogenic differentiation can be observed with synthesis of a calcified matrix. These experimental data are fully consistent with the previous description of osteoid matrix in a subgroup of *EWS-FLI1*-positive tumors called small cell osteosarcoma (Oshima et al., 2004). A less evident commitment of *EWS-FLI1* silenced cells toward the chondrogenic lineage is also observed. Despite the death of Ewing cells observed upon chondrocyte differentiation conditions, impairing the evaluation of the terminal differentiation, *COL10A1, SOX9 and RUNX2*, three markers suggestive of a commitment toward the chondrocyte lineage are induced upon *EWS-FLI1* silencing. *SOX9* can be induced in chondrogenic but also in neural differentiation. To further investigate the hypothesis of *SOX9* induction being related to differentiation along the neural lineage, we also analyzed the expression of *SNAI2*, *FOXD3* and *PAX7*, three markers which are required for neural crest cells differentiation (Basch et al., 2006). *PAX7* was strongly (10X) inhibited by *EWS-FLI1* silencing. *FOXD3* and *SNAI2* were slightly inhibited or induced, respectively. Interestingly, none of these markers were induced upon treatment of Ewing cells with DMSO/HBA or DMSO/RA, two protocols previously described for neural differentiation (Scintu et al., 2006; Woodbury et al., 2002; Woodbury et al., 2000).

These results strongly suggest that the *SOX9* induction is rather related to a chondrocyte than a neural commitment.

Altogether, these *in silico* and experimental data strongly suggest that Ewing cells arise from MSC which terminal mesenchymal differentiation is blocked by *EWS-FLI1*. It also shows that the phenotype of Ewing cells is perverted from the mesenchymal to neural lineage by *EWS-FLI1.* However, some Ewing cell lines (SK-N-MC), despite a strong convergence toward a MSC gene expression profile upon *EWS-FLI1* silencing do not differentiate, at least along the adipogenic lineage. This indicates that the Ewing cell background, although related to MSC, harbor cell line-specific differences which may reflect diverse mesenchymal potentials of the original progenitors in which the *EWS-FLI1* fusion occurred. Alternatively, some Ewing cell lines may have acquired secondary genetic changes impairing differentiation processes.

The MSCs compartment consists of heterogeneous population of cells and presently, no single marker can be used to isolate subpopulations of MSCs committed to specific lineages. Stem cells with an extended differentiation potential, in particular in the angiogenic lineage, can be isolated from adipose tissue and bone marrow. In that respect, it is striking that different genes involved in angiogenesis are modulated by *EWS-FLI1*. The hypothesis of a vascular differentiation potential of ET cells, which was proposed by James Ewing himself, is further supported by recent microarray data and by the observation of vascular mimicry in ET associated with the ability of some Ewing cell lines to form vascular-like tubes *in vitro* (Staege et al., 2004; van der Schaft et al., 2005). In that respect, it is interesting to mention that *FLI1*, the wild type counterpart of *EWS-FLI1*, is a key regulator of early blood vessel formation (Brown et al., 2000). Taken together, *in silico* and experimental results

suggest that ETs are derived from MSCs that may have both mesenchymal and vascular potentials. ET may therefore constitute an appropriate model to further study the characteristics of a common mesenchymal and vascular progenitor.

The identification of the Ewing primary cell constitutes a key step toward a better understanding of ET biology. The MSC origin may account for the predominant localization of ET in bones or soft tissues, two major sources for these stem cells. Through a precise spatio-temporal targeting of *EWS-FLI1* expression in the mouse, it should foster the development of a Ewing tumor model, which is presently lacking and which may be of considerable help to achieve comprehensive insights into tumor initiation and progression processes.

Acknowledgments

We thank Zofia Maciorowski from the department of tumor biology of the Institut Curie for the BrdU analyses, Hans Clevers for the generous gift of the pTER and the Tet repressor expression plasmid (pTet-R) and Pierre Charneau for providing us the pTRIP lentivirus. We also thank Gilbert Lenoir and Steve Lessnick for materials used in this study. This work was supported by grants from the Institut National de la Santé et de la Recherche Médicale, the Institut Curie, the Ligue Nationale contre le Cancer (Equipe labellisée and CIT program), the Réseau National des Génopoles and the Association for International Cancer Research (AICR).

Figure legends

Figure 1. *EWS-FLI1*-silenced Ewing cells profiles converge toward a mesenchymal stem cell expression pattern.

(A) Principal component analysis comparing the gene expression profiles of *EWS-FLI1*-silenced (efRNAi) and control (ctrlRNAi) A673, EW24 and SK-N-MC Ewing cell lines, Ewing tumors (ET), mesenchymal stem cells (MSC) and various tissues, using the whole transcriptome data. Mesench.: differentiated mesenchymal tissues (smooth muscle, adipocytes), Hemato: Hematopoietic tissues, Epith: Epithelial tissues. The precise description of these tissues is provided in Table S1. Each plotted data point represents a single profile. In particular, individual data points for inhibition of *EWS-FLI1* by RNA interference are shown.

(B) Same analysis than in (A) but performed with *EWS-FLI1*-modulated probe sets (SAM analyses between efRNAi and ctrlRNAi samples, absolute fold change >3; q-value <0.01). The two first components account for 41.8% of the variation.

(C) Hierarchical clustering analysis (average linkage method, 1- rank correlation distance metric) using *EWS-FLI1*-modulated probe sets. efRNAi samples cluster with mesenchymal tissues and stem cells. The complete annotated cluster is provided as Figure S1.

(D) A significant proportion of genes differentially expressed between efRNAi and ctrlRNAi also distinguishes MSCs from ET. The blue circle schematizes the set of genes exhibiting significant variation (>2 fold; q-value<0.01) between *EWS-FLI1*-silenced or -expressing Ewing cells (efRNAi/ctrlRNAi) and the red circle represents the set of genes differentially expressed between MSCs and ETs (the complete list of genes is provided in Table S2). The table represents the distribution of the 110 genes found in the overlap. 99 genes behave consistently between MSC/ET and

ef/ctrlRNAi: 44 genes upregulated in MSCs as compared to ETs are downregulated by *EWS-F*LI1 and 55 genes downregulated in MSCs as compared to ETs are upregulated by *EWS-FLI1*.

(E) Venn diagram showing, among the 2540 genes which discriminates MSCs and ETs, the number of genes regulated by *EWS-FLI1* in a cell line specific manner. For each cell line, the number of *EWS-FLI1*-modulated genes (Welch test p-value<0.01, absolute fold change >2) common with the gene set of the MSC/ET comparison is represented. Among the 782, 364 and 382 genes regulated by *EWS-FLI1* in A673, EW24 or SK-N-MC, 320, 93 and 82 are common with the MSC/ET comparison, respectively.

Figure 2. Differentiation of *EWS-FLI1*-silenced EW24 cells along the adipogenic lineage.

(A) Quantitative RT-PCR analysis of specific adipocyte markers on EW24 cells infected by the *EWS-FLI1* specific (shEF1) or control (shCT) lentiviruses grown in either standard (-) or differentiation medium (Diff). The mean values and standard deviation obtained for duplicate experiments are indicated.

(B) Oil-Red-O staining of EW24 cells infected with shCT or shEF1-encoding lentiviruses and cultured in standard (-) or adipogenic conditions (diff).

Figure 3. Long term silencing of *EWS-FLI1* induces mesenchymal features.

(A) Temporal analysis of *EWS-FLI1* mRNA (left panel) and protein (right panel) expression upon doxycycline treatment of shA673 cells. β-actin is used as a control. For mRNA expression, the mean values +/- SD obtained for duplicate experiments are indicated.

(B) Quantitative RT-PCR analysis of the specific adipocyte markers on shA673 induced (+DOX) or not (-DOX) by 1µg/mL of doxycyclin in either standard (-) or

differentiation medium (Diff). The mean values +/- SD obtained for duplicate experiments on both shA673 clones are indicated.

(C) Oil-Red-O staining of shA673-1C cultured in standard (-) or adipogenic conditions (diff) in the absence or presence of DOX.

(D) Quantitative RT-PCR analysis of specific osteocyte and chondrocyte markers. The mean values +/- SD obtained for duplicate experiments on both shA673 clones are indicated.

(E) Von-Kossa staining of the mineralized matrix for shA673-1C cultured in standard (-) or osteogenic differentiation (diff) conditions in the presence or absence of DOX.

(F) FACS analyses of four cell surface markers (CD59, CD73, CD54 and CD44). Cells were treated (black lines) or not (grey lines) with DOX during 6 days prior to FACS analyses. Dashed lines represent control IgE.

References

Arvand, A., and Denny, C. T. (2001). Biology of EWS/ETS fusions in Ewing's family tumors. Oncogene *20*, 5747-5754.

Basch, M. L., Bronner-Fraser, M., and Garcia-Castro, M. I. (2006). Specification of the neural crest occurs during gastrulation and requires Pax7. Nature *441*, 218-222.

Boquest, A. C., Shahdadfar, A., Fronsdal, K., Sigurjonsson, O., Tunheim, S. H., Collas, P., and Brinchmann, J. E. (2005). Isolation and transcription profiling of purified uncultured human stromal stem cells: alteration of gene expression after in vitro cell culture. Mol Biol Cell *16*, 1131-1141.

Brown, L. A., Rodaway, A. R., Schilling, T. F., Jowett, T., Ingham, P. W., Patient, R. K., and Sharrocks, A. D. (2000). Insights into early vasculogenesis revealed by expression of the ETS-domain transcription factor Fli-1 in wild-type and mutant zebrafish embryos. Mech Dev *90*, 237-252.

Castillero-Trejo, Y., Eliazer, S., Xiang, L., Richardson, J. A., and Ilaria, R. L., Jr. (2005). Expression of the EWS/FLI-1 oncogene in murine primary bone-derived cells Results in EWS/FLI-1-dependent, ewing sarcoma-like tumors. Cancer research *65*, 8698-8705.

Cavazzana, A. O., Miser, J. S., Jefferson, J., and Triche, T. J. (1987). Experimental evidence for a neural origin of Ewing's sarcoma of bone. Am J Pathol *127*, 507-518.

Chansky, H. A., Barahmand-Pour, F., Mei, Q., Kahn-Farooqi, W., Zielinska-Kwiatkowska, A., Blackburn, M., Chansky, K., Conrad, E. U., 3rd, Bruckner, J. D., Greenlee, T. K., and Yang, L. (2004). Targeting of EWS/FLI-1 by RNA interference attenuates the tumor phenotype of Ewing's sarcoma cells in vitro. J Orthop Res *22*, 910-917.

Covas, D. T., Piccinato, C. E., Orellana, M. D., Siufi, J. L., Silva, W. A., Jr., Proto-Siqueira, R., Rizzatti, E. G., Neder, L., Silva, A. R., Rocha, V., and Zago, M. A. (2005). Mesenchymal stem cells can be obtained from the human saphena vein. Experimental cell research *309*, 340-344.

Dauphinot, L., De Oliveira, C., Melot, T., Sevenet, N., Thomas, V., Weissman, B. E., and Delattre, O. (2001). Analysis of the expression of cell cycle regulators in Ewing cell lines: EWS-FLI-1 modulates p57KIP2and c-Myc expression. Oncogene *20*, 3258-3265.

Delattre, O., Zucman, J., Plougastel, B., Desmaze, C., Melot, T., Peter, M., Kovar, H., Joubert, I., de Jong, P., Rouleau, G., and et al. (1992). Gene fusion with an ETS DNA-binding domain caused by chromosome translocation in human tumours. Nature *359*, 162-165.

Dennis, J. E., and Charbord, P. (2002). Origin and differentiation of human and murine stroma. Stem Cells *20*, 205-214.

Eliazer, S., Spencer, J., Ye, D., Olson, E., and Ilaria, R. L., Jr. (2003). Alteration of mesodermal cell differentiation by EWS/FLI-1, the oncogene implicated in Ewing's sarcoma. Molecular and cellular biology *23*, 482-492.

Ewing, J. (1921). Diffuse endothelioma of bone. Proc New York Pathol Soc *21*, 17-24.

Friedenstein, A. J., Gorskaja, J. F., and Kulagina, N. N. (1976). Fibroblast precursors in normal and irradiated mouse hematopoietic organs. Exp Hematol *4*, 267-274.

Gregory, C. A., Prockop, D. J., and Spees, J. L. (2005). Non-hematopoietic bone marrow stem cells: molecular control of expansion and differentiation. Experimental cell research *306*, 330-335.

Hu-Lieskovan, S., Zhang, J., Wu, L., Shimada, H., Schofield, D. E., and Triche, T. J. (2005). EWS-FLI1 fusion protein up-regulates critical genes in neural crest development and is responsible for the observed phenotype of Ewing's family of tumors. Cancer research *65*, 4633-4644.

Izadpanah, R., Joswig, T., Tsien, F., Dufour, J., Kirijan, J. C., and Bunnell, B. A. (2005). Characterization of multipotent mesenchymal stem cells from the bone marrow of rhesus macaques. Stem Cells Dev *14*, 440-451.

Janknecht, R. (2005). EWS-ETS oncoproteins: the linchpins of Ewing tumors. Gene *363*, 1-14.

Johnstone, B., Hering, T. M., Caplan, A. I., Goldberg, V. M., and Yoo, J. U. (1998). In vitro chondrogenesis of bone marrow-derived mesenchymal progenitor cells. Experimental cell research *238*, 265-272.

Kiepe, D., Ciarmatori, S., Haarmann, A., and Tonshoff, B. (2006). Differential expression of IGF system components in proliferating vs. differentiating growth plate chondrocytes: the functional role of IGFBP-5. American journal of physiology *290*, E363-371.

Noguera, R., Navarro, S., Peydro-Olaya, A., and Llombart-Bosch, A. (1994). Patterns of differentiation in extraosseous Ewing's sarcoma cells. An in vitro study. Cancer *73*, 616-624.

Oshima, Y., Kawaguchi, S., Nagoya, S., Wada, T., Kokai, Y., Ikeda, T., Nogami, S., Oya, T., and Hirayama, Y. (2004). Abdominal small round cell tumor with osteoid and EWS/FLI1. Human pathology *35*, 773-775.

Oswald, J., Boxberger, S., Jorgensen, B., Feldmann, S., Ehninger, G., Bornhauser, M., and Werner, C. (2004). Mesenchymal stem cells can be differentiated into endothelial cells in vitro. Stem Cells *22*, 377-384.

Parkinson, H., Sarkans, U., Shojatalab, M., Abeygunawardena, N., Contrino, S., Coulson, R., Farne, A., Lara, G. G., Holloway, E., Kapushesky, M., *et al.* (2005). ArrayExpress--a public repository for microarray gene expression data at the EBI. Nucleic Acids Res *33*, D553-555.

Pittenger, M. F., Mackay, A. M., Beck, S. C., Jaiswal, R. K., Douglas, R., Mosca, J. D., Moorman, M. A., Simonetti, D. W., Craig, S., and Marshak, D. R. (1999). Multilineage potential of adult human mesenchymal stem cells. Science *284*, 143-147.

Prieur, A., Tirode, F., Cohen, P., and Delattre, O. (2004). EWS/FLI-1 silencing and gene profiling of Ewing cells reveal downstream oncogenic pathways and a crucial role for repression of insulin-like growth factor binding protein 3. Molecular and cellular biology *24*, 7275-7283.

R Development Core Team, ed. (2005). R: A language and environment for statistical computing., (Vienna, Austria.).

Riggi, N., Cironi, L., Provero, P., Suva, M. L., Kaloulis, K., Garcia-Echeverria, C., Hoffmann, F., Trumpp, A., and Stamenkovic, I. (2005). Development of Ewing's sarcoma from primary bone marrow-derived mesenchymal progenitor cells. Cancer research *65*, 11459-11468.

Rorie, C. J., Thomas, V. D., Chen, P., Pierce, H. H., O'Bryan, J. P., and Weissman, B. E. (2004). The Ews/Fli-1 fusion gene switches the differentiation program of neuroblastomas to Ewing sarcoma/peripheral primitive neuroectodermal tumors. Cancer research *64*, 1266-1277.

Saeed, A. I., Sharov, V., White, J., Li, J., Liang, W., Bhagabati, N., Braisted, J., Klapa, M., Currier, T., Thiagarajan, M., *et al.* (2003). TM4: a free, open-source system for microarray data management and analysis. BioTechniques *34*, 374-378.

Schuetz, A. N., Rubin, B. P., Goldblum, J. R., Shehata, B., Weiss, S. W., Liu, W., Wick, M. R., and Folpe, A. L. (2005). Intercellular junctions in Ewing sarcoma/primitive neuroectodermal tumor: additional evidence of epithelial differentiation. Mod Pathol *18*, 1403-1410.

Schutze, N., Noth, U., Schneidereit, J., Hendrich, C., and Jakob, F. (2005). Differential expression of CCN-family members in primary human bone marrow-derived mesenchymal stem cells during osteogenic, chondrogenic and adipogenic differentiation. Cell Commun Signal *3*, 5.

Scintu, F., Reali, C., Pillai, R., Badiali, M., Sanna, M. A., Argiolu, F., Ristaldi, M. S., and Sogos, V. (2006). Differentiation of human bone marrow stem cells into cells with a neural phenotype: diverse effects of two specific treatments. BMC neuroscience [electronic resource] *7*, 14.

Smith, R., Owen, L. A., Trem, D. J., Wong, J. S., Whangbo, J. S., Golub, T. R., and Lessnick, S. L. (2006). Expression profiling of EWS/FLI identifies NKX2.2 as a critical target gene in Ewing's sarcoma. Cancer cell *9*, 405-416.

Staege, M. S., Hutter, C., Neumann, I., Foja, S., Hattenhorst, U. E., Hansen, G., Afar, D., and Burdach, S. E. (2004). DNA microarrays reveal relationship of Ewing family tumors to both endothelial and fetal neural crest-derived cells and define novel targets. Cancer research *64*, 8213-8221.

Su, A. I., Wiltshire, T., Batalov, S., Lapp, H., Ching, K. A., Block, D., Zhang, J., Soden, R., Hayakawa, M., Kreiman, G.*, et al.* (2004). A gene atlas of the mouse and human protein-encoding transcriptomes. Proc Natl Acad Sci U S A *101*, 6062-6067.

Torchia, E. C., Jaishankar, S., and Baker, S. J. (2003). Ewing tumor fusion proteins block the differentiation of pluripotent marrow stromal cells. Cancer research *63*, 3464-3468.

Tusher, V. G., Tibshirani, R., and Chu, G. (2001). Significance analysis of microarrays applied to the ionizing radiation response. Proc Natl Acad Sci U S A *98*, 5116-5121.

van de Wetering, M., Oving, I., Muncan, V., Pon Fong, M. T., Brantjes, H., van Leenen, D., Holstege, F. C., Brummelkamp, T. R., Agami, R., and Clevers, H. (2003). Specific inhibition of gene expression using a stably integrated, inducible small-interfering-RNA vector. EMBO Rep *4*, 609-615.

van der Horst, G., van der Werf, S. M., Farih-Sips, H., van Bezooijen, R. L., Lowik, C. W., and Karperien, M. (2005). Downregulation of Wnt signaling by increased expression of Dickkopf-1 and -2 is a prerequisite for late-stage osteoblast differentiation of KS483 cells. J Bone Miner Res *20*, 1867-1877.

van der Schaft, D. W., Hillen, F., Pauwels, P., Kirschmann, D. A., Castermans, K., Egbrink, M. G., Tran, M. G., Sciot, R., Hauben, E., Hogendoorn, P. C.*, et al.* (2005). Tumor cell plasticity in Ewing sarcoma, an alternative circulatory system stimulated by hypoxia. Cancer research *65*, 11520-11528.

Woodbury, D., Reynolds, K., and Black, I. B. (2002). Adult bone marrow stromal stem cells express germline, ectodermal, endodermal, and mesodermal genes prior to neurogenesis. Journal of neuroscience research *69*, 908-917.

Woodbury, D., Schwarz, E. J., Prockop, D. J., and Black, I. B. (2000). Adult rat and human bone marrow stromal cells differentiate into neurons. Journal of neuroscience research *61*, 364-370.

Zucman, J., Melot, T., Desmaze, C., Ghysdael, J., Plougastel, B., Peter, M., Zucker, J. M., Triche, T. J., Sheer, D., Turc-Carel, C., and et al. (1993). Combinatorial generation of variable fusion proteins in the Ewing family of tumours. EMBO J *12*, 4481-4487.

Table 1. Main genes modulated by EWS-FLI-1 and differentially expressed between MSC and ET

Symbol	ET/MSC	A673[a]	SKNMC[a]	EW24[a]	Symbol	ET/MSC	A673[a]	SKNMC[a]	EW24[a]
Mesenchymal differentiation					**Extracellular matrix and cytoskeleton**				
CALD1	-13.8	-3.5	-3.4	-3.2	ARHGAP29	-22.1	-4.9	-2.8	-5.2
CYR61	-21.3	-6.0	-10.7	-11.6	ITGB5	-10.9	-2.7		-2.9
DKK1	-2.2	-33.7	-11.5	-24.3	MARCKS	-4.1	-2.2		-2.2
IGFBP5	-7.0	-25.8	-8.7	-8.5	MID1	-29.7		-2.0	-2.6
IGFBP7	-3.8	-29.8	-17.9	-18.9	PALLD	-11.3	-2.4	-2.7	-3.4
PPP1R1A	152.9	12.9		4.8	PLAT	-26.5	-11.1		-2.1
PRKCB1	236.4	17.4	3.1	2.7	RND3	-91.5	-23.2	-4.6	-8.7
PTGER3	23.2	2.8	4.1	2.7	S100A10	-5.3	-5.6	-4.7	-4.2
SPARC	-3.1	-3.3	-4.2	-4.9	SDC2	-29.1	-2.0	-5.2	-5.6
TPM1	-8.2	-13.7	-5.8	-5.8	SPTBN1	-7.9		-2.3	-2.5
VDAC1	10.2		11.7	8.8	VCL	-4.9	-2.5	-2.7	-3.9
Neurogenesis					**Angiogenesis**				
ATP2B1	-5.4	-2.2		-5.2	ADM	-108.1	-23.1	-37.1	-47.9
JARID2	4.5		2.4	2.9	CYR61	-21.3	-6.0	-10.7	-11.6
NKX2-2	341.0	29.8	2.7		TFPI	-20.1	-6.1	-3.1	-2.3
NLGN4X	29.3		2.2	2.9	TNFRSF12A	-3.9	-2.2	-3.6	-2.9
OLFM1	39.3	5.6	2.5	2.4					
PRNP	-2.4	-5.8		-2.0					
RCOR1	8.9	6.6	5.0						

[a] Mean fold change between ctrlRNAi and efRNAi samples. - indicates *EWS/FLI-1*-repressed genes.

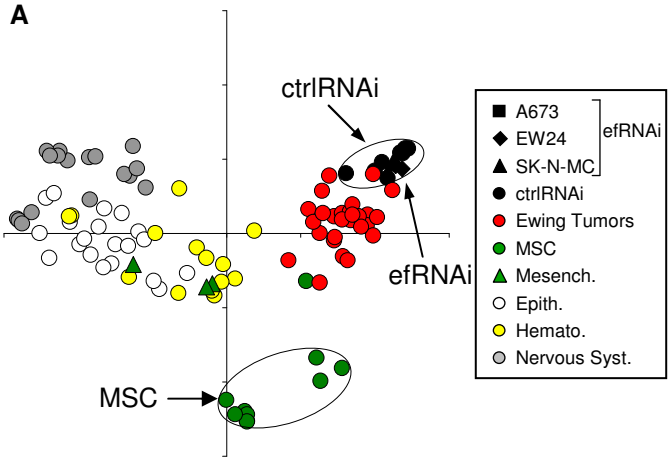

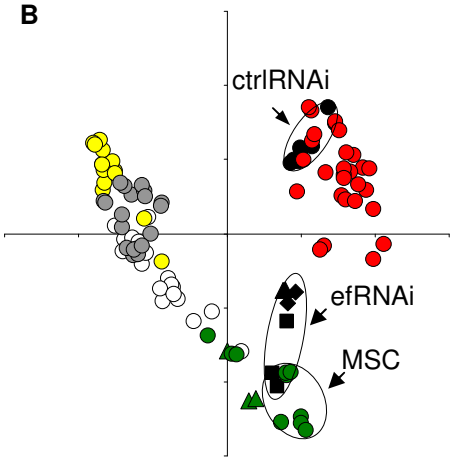

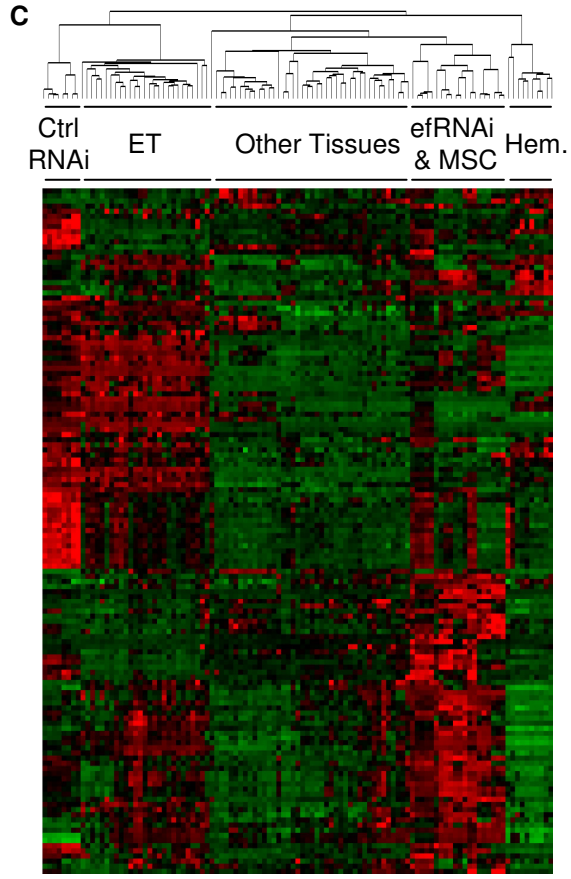

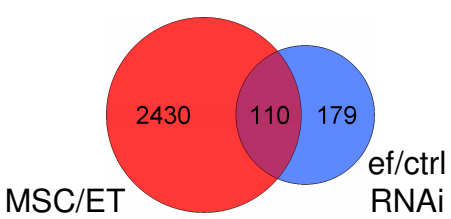

ctrl/efRNAi / MSC/ET	EWS-FLI1	
	Up regulated	Down regulated
Overexpressed in MSC	9	44
Underexpressed in MSC	55	2

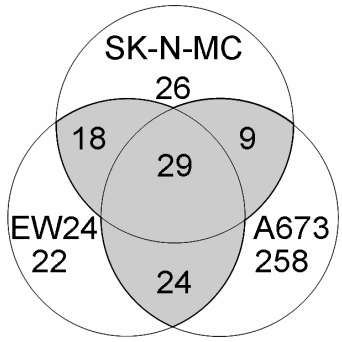

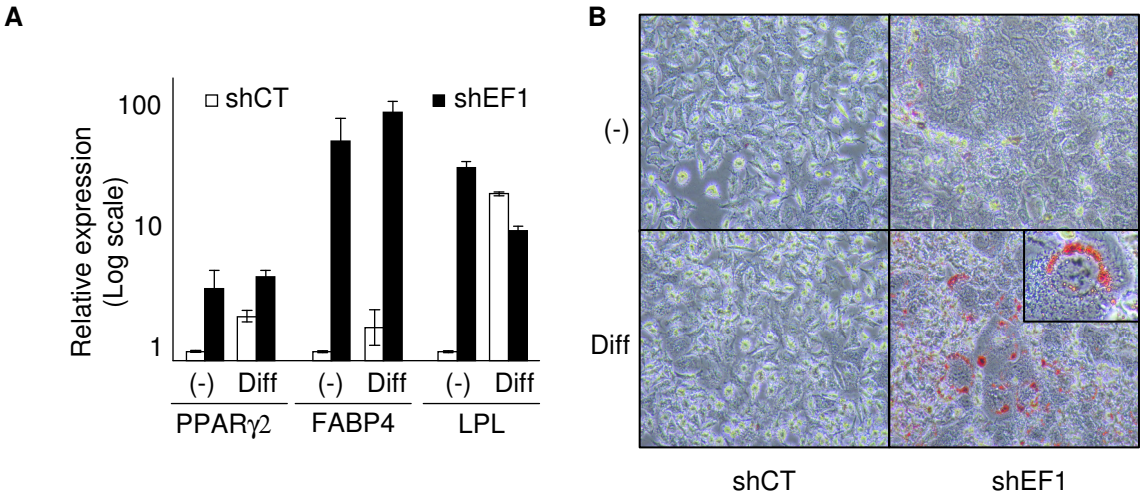
A
B
shCT
shEF1
Relative expression
(Log scale)
100
10
1
(-)
Diff
PPARγ2
FABP4
LPL
shCT
shEF1

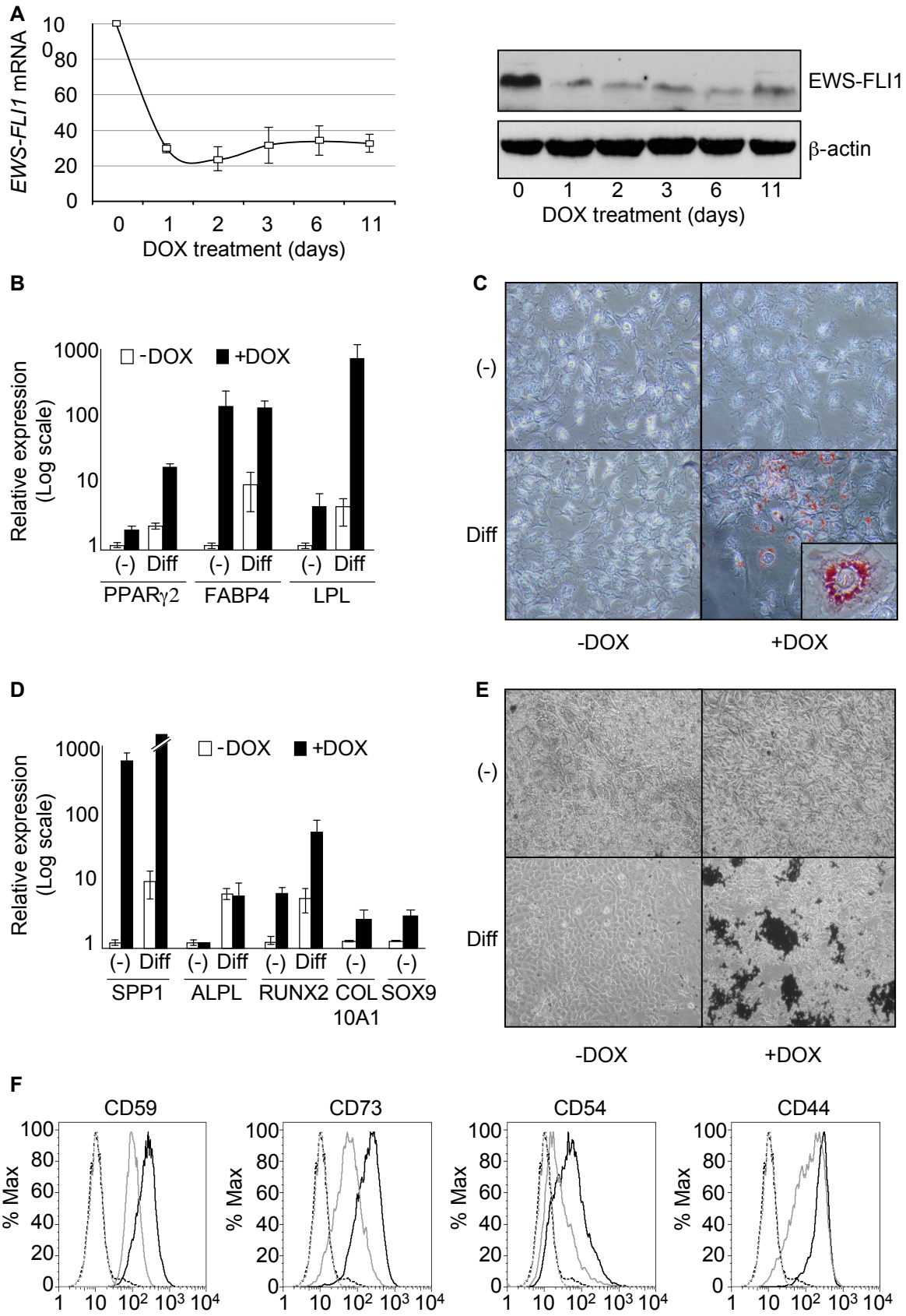
A
EWS-FLI1 mRNA
10
0
80
60
40
20
0
0 1 2 3 6 11
DOX treatment (days)
EWS-FLI1
β-actin
0 1 2 3 6 11
DOX treatment (days)
B
Relative expression (Log scale)
1000
100
10
1
-DOX
+DOX
(-) Diff (-) Diff (-) Diff
PPARγ2
FABP4
LPL
C
(-)
Diff
-DOX
+DOX
D
Relative expression (Log scale)
1000
100
10
1
-DOX
+DOX
(-) Diff (-) Diff (-) Diff (-) (-)
SPP1
ALPL
RUNX2
COL 10A1
SOX9
E
(-)
Diff
-DOX
+DOX
F
CD59
CD73
CD54
CD44
% Max
100
80
60
40
20
0
1 10 10² 10³ 10⁴